Materials Research, Vol. 9, No. 4, 375-379, 2006

Effect of Rare Earth Oxide Additions on Oxidation Behavior of AISI 304L Stainless Steel

Marina Fuser Pillis, Edval Gonçalves de Araújo, Lalgudi Venkataraman Ramanathan*

Materials Science and Technology Center, Instituto de Pesquisas Energéticas e Nucleares, Av. Prof. Lineu Prestes, 2242, Cidade Universitária, 05508-000 São Paulo - SP, Brazil

Received: February 1, 2006; Revised: October 24, 2006

AISI 304L stainless steel powder compacts containing 2 vol% high purity rare earth oxides were prepared by mixing the different powders in a vibratory mill followed by pressing. The compacts thus obtained were sintered in a vacuum furnace and isothermal oxidation measurements were carried out in a muffle furnace, in air, up to 200 hours at 900 °C. The oxidized surfaces were examined in a scanning electron microscope and micro regions of the reaction products were studied using energy dispersive analysis. The addition of rare earth oxides decreased the oxidation rate of the stainless steel. Further evidence of predominant oxygen ion diffusion controlling the overall oxidation process in rare earth containing chromium oxide forming alloys has been observed.

Keywords: *rare earth elements, oxidation, high temperature*

1. Introduction

Alloys for use at high temperatures should have adequate mechanical strength and resistance to chemical degradation caused by reactions between the alloy and the environment[1,2]. Most structural alloys are Fe, Ni or Co based alloys and the oxides formed on their surfaces are not sufficiently protective above 550 °C. Therefore these alloys contain Cr and/or Al to form more protective oxide scales of chromium oxide or alumina respectively[3]. The addition of other reactive elements such as yttrium, zirconium or cerium, to these alloys improves the protective properties of the surface oxides even more[4-8]. Rare earth (RE) oxides in the form of dispersions have also been added to these alloys to form protective surface oxides[9]. Various mechanisms have been proposed to explain the improvements in oxidation resistance brought about by addition of RE elements or their oxides. The mechanism most widely accepted attributes the improvements to diffusion of the RE ions to oxide grain boundaries and blocking of alloy cation diffusion from the metal/oxide to the oxide/air interface[10]. This paper presents the effect of neodymium, yttrium, lanthanum and ytterbium oxide additions on oxidation behavior of AISI 304L stainless steel.

2. Materials and Methods

Powders of AISI 304L (0.01 C, 0.01 S, 11.3 Ni, 19.1 Cr, 0.9 Si, 0.159 O, 0.056 N, 0.2 Mn and balance Fe) and 2 vol.% high purity oxides of neodymium, ytterbium, lanthanum and yttrium were mixed for 1 hour in a vibratory mill to obtain the powder mix. This powder mix was compacted in a uniaxial press and the compacts sintered in vacuum for 1 hour at 1250 °C. Specimens of the compacts for optical microscopy were polished and etched by immersion for 5 seconds in a solution containing 30 mL hydrochloric acid and 20 mL ethanol. Isothermal oxidation was carried out in a muffle furnace for 200 hours at 900 °C. Weight gains *vs.* time curves were obtained and the weight gains took into account the weight of the spalled oxide, where pertinent. The surfaces and cross sections of specimens oxidized for 20 hours and 200 hours were examined in a scanning electron microscope and energy dispersive spectroscopic analysis of micro-regions carried out.

3. Results and Discussion

The hydrostatic density of the various sintered materials did not vary much and was in the range 86.2 to 89.1% of the theoretical density.

Figure 1 shows micrographs of longitudinal sections of sintered AISI 304L. Neck formation between alloy particles and irregular shaped pores can be seen in Figure 1a. Twinned austenite grains are shown in Figure 1b. The cross-section and longitudinal section of the Yb_2O_3 containing specimen are shown in Figure 2a and b. Embedded RE oxide particles at metal particle interfaces(arrows) and twinned austenite grains can be observed.

The weight gain *vs.* time curves of specimens oxidized in the muffle furnace are shown in Figure 3. Addition of RE oxides decreased the overall weight gain compared to the stainless steel without any additions. After 20 hours at 900 °C, none of the specimens spalled. After 50 hours, among all the samples, only the oxides on specimens without RE additions and with Y_2O_3 started spalling. Oxide spalling on Y_2O_3 containing specimen was slight and in the form of a fine powder, where as that on the specimen without additions of RE oxides was in the form of large scales. During the first 20 hours of oxidation, the effect of adding the different RE oxides was similar.

Figure 4a shows the surface of AISI 304L oxidized for 20 hours. Acicular oxides can be seen in region 1 and this was rich in Fe and Ni. Region 2 was rich in Fe and contained traces of Cr and Ni. A cross-section of the same material is shown in Figure 4b and an irregular oxide layer is seen. The oxide/metal interface is undulating and regions with internal oxidation can also be observed besides cracks and pores. The outer part of the oxide layer (region 1) consists essentially of Fe and some Cr. In the lighter intermediate region (region 2), Ni was also observed. The internal oxidation zone (region 3) revealed Cr and Ni, and region 4, close to the metal/oxide interface was rich in Cr.

The surface of AISI 304L oxidized for 200 hours is shown in Figure 5a. The specimens revealed severe spalling. Oxides with varying morphologies can be observed. EDS analysis revealed that in spite of the differing morphologies, they were all rich in Fe. In the oxides shown with numbers 1 and 2, small quantities of Cr was detected, and in the oxide shown with number 3, besides Fe and Cr, Ni was also present. Figure 5b shows a region of the oxide that was still adhering

*e-mail: mfpillis@ipen.br
Article presented at the 4th International Latin-american conference on Powder Technology, November 19-21, Guarujá, São Paulo, 2003, Brazil

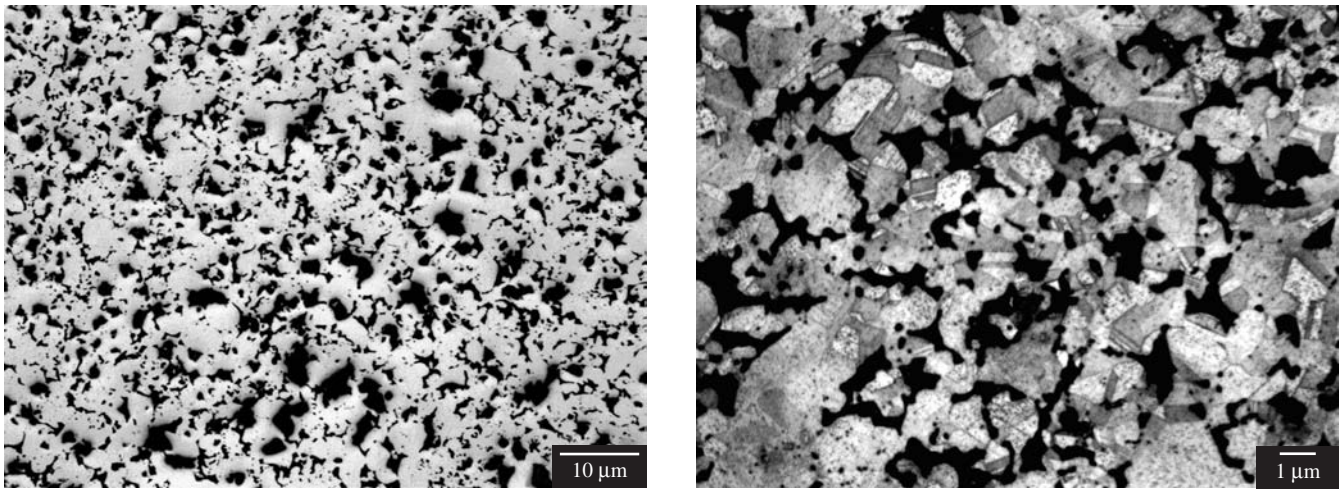

(a) (b)

Figure 1. Longitudinal sections of sintered AISI 304L. a) not etched; and b) etched.

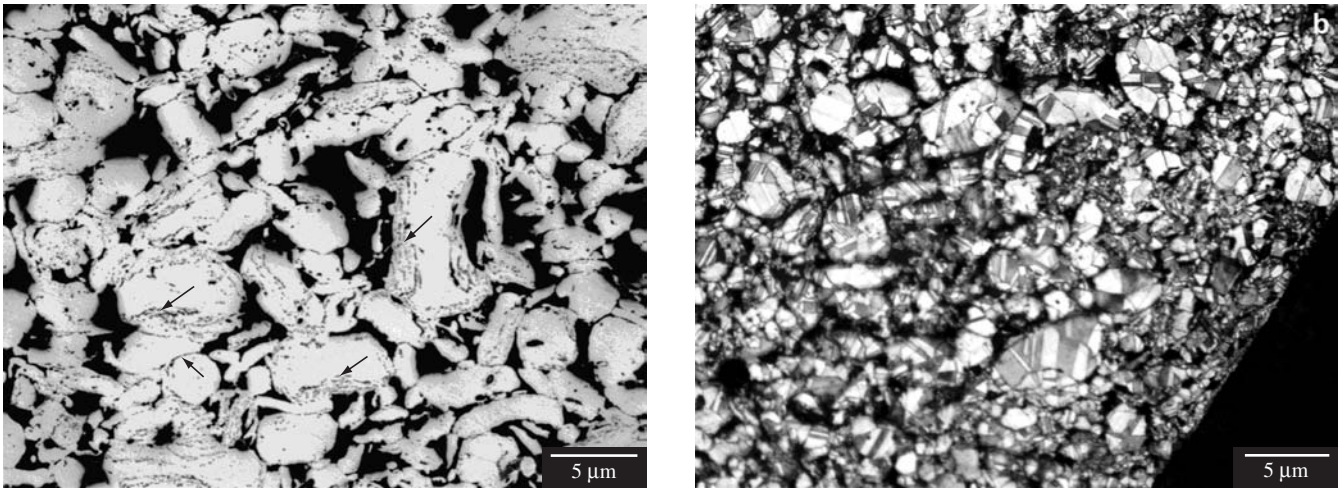

(a) (b)

Figure 2. Microstructure of sintered AISI 304L + Yb_2O_3. a) cross-section without etching; and b) longitudinal section etched.

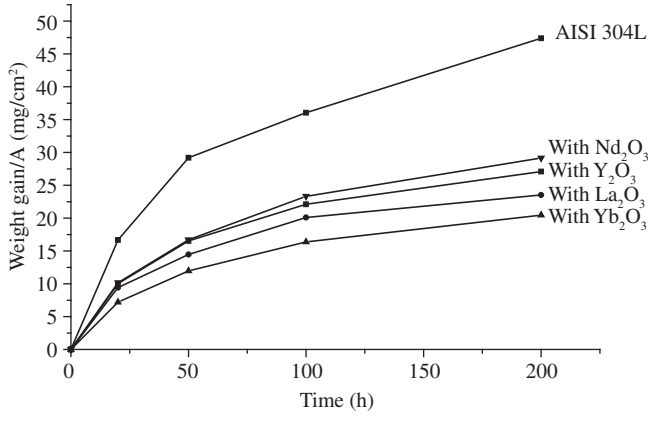

Figure 3. Oxidation Curves at 900 °C.

to the alloy and revealed high Cr content. The cross section of the same material is shown in Figure 5c and high Fe with traces of Cr was noted in region 1 and high Ni in region 2. Figure 5d is a higher magnification micrograph of a part of the oxide still adhering to the base metal and it reveals zones of internal oxidation. Region 1 was found to be rich in Cr and Fe, region 2 contained high Ni besides Cr and Fe and region 3, revealed large amounts of Cr and Fe.

Figure 6a presents the surface of Yb_2O_3 containing AISI304L oxidized for 20 hours. The light colored regions are Yb_2O_3. The morphology of the oxide formed on the surface is quite distinct from that formed on the RE oxide free steel (Figure 4a). Figure 6b is a cross section of the same material and reveals an oxide layer that is thinner than that formed on RE oxide free steel. Pores can also be observed in the oxide. The light regions within the oxide layer were identified as Yb_2O_3 particles and serve as a marker, indicating the oxide growth direction, that is, towards the alloy. This lends further proof to oxide growth mechanism in the presence of RE being by anion diffusion. On the outer regions of the oxide, close to the oxide/gas interface, indicated in the micrograph as 1, Cr and Ni were detected, besides Fe. In the intermediate lighter region 2, the Ni level was higher and in region 3, close to the oxide/metal interface, the Cr level was high. Region 4 is a Yb_2O_3 agglomerate.

The surface and cross section of AISI 304L + Yb_2O_3 oxidized for 200 hours are shown in Figures 7a and 7b. Region 1, close to the oxide/gas interface showed only Fe and region 2, large amounts of Ni and Cr, besides Fe. The intermediate light region 3, was rich in Ni

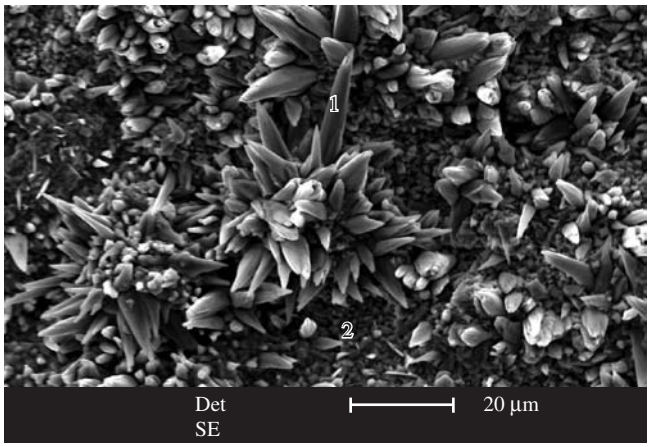

(a)

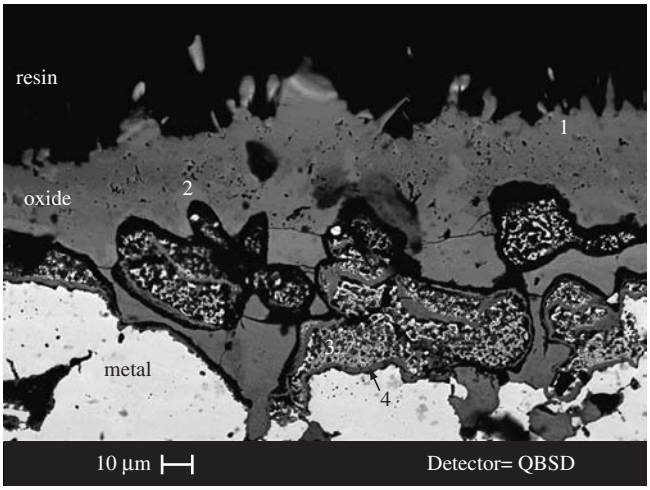

(b)

Figure 4. AISI 304L oxidized for 20 hours at 900 °C. a) surface; b) cross-section.

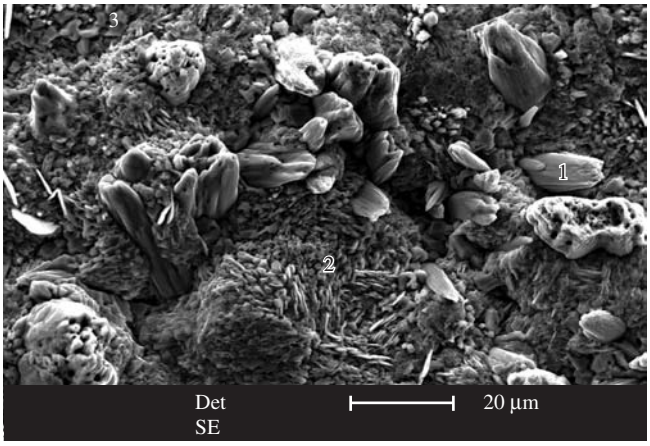

(a)

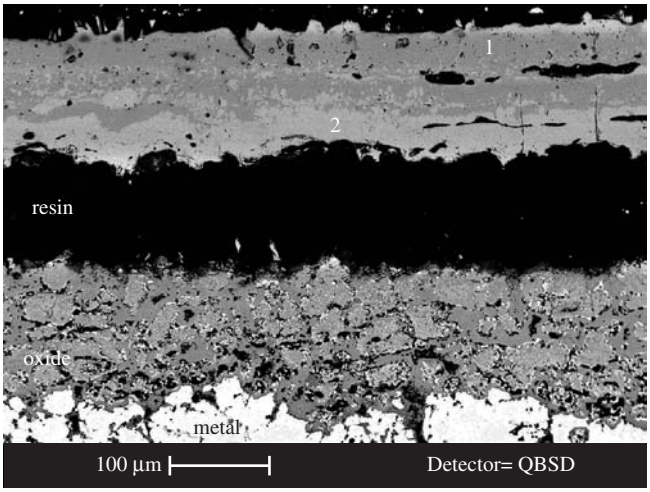

(c)

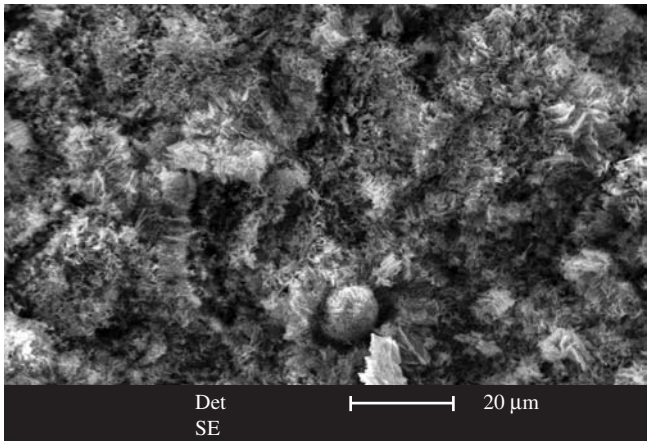

(b)

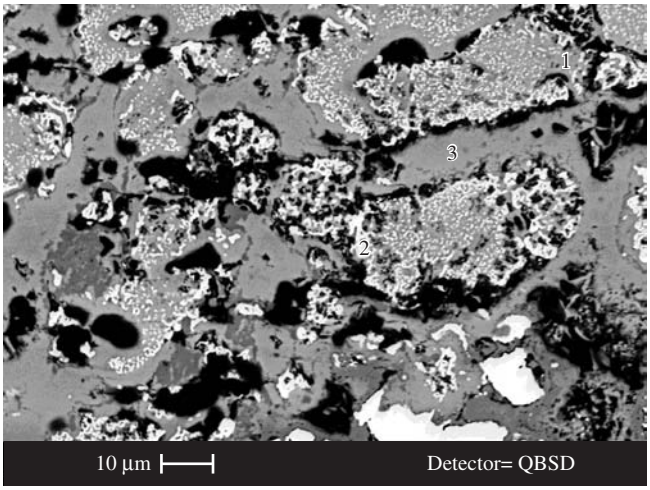

(d)

Figure 5. AISI 304L oxidized for 200 hours at 900 °C. a) surface (not spalled region); b) surface (spalled region); c) cross-section; and d) higher magnification in a region of (c).

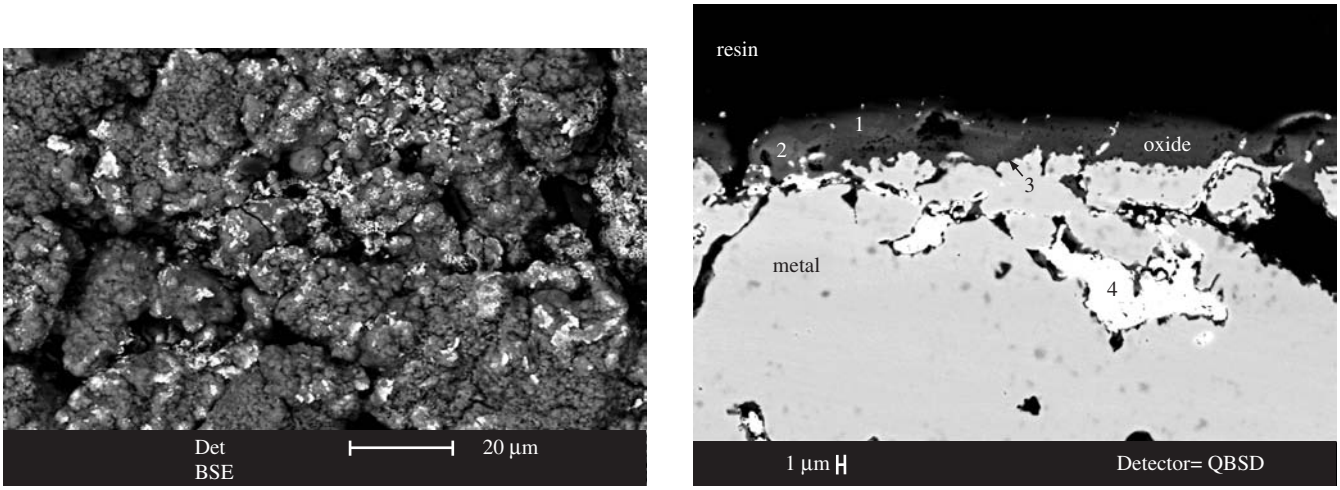

(a) (b)

Figure 6. AISI 304L + Yb_2O_3 oxidized for 20 hours at 900 °C. a) surface; and b) cross-section.

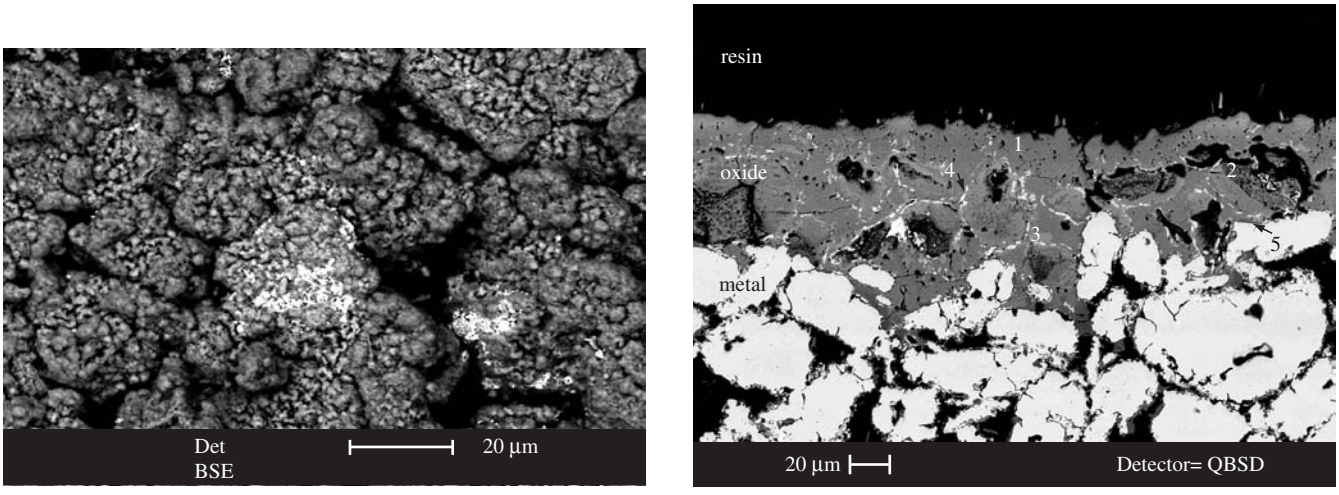

(a) (b)

Figure 7. AISI 304L + Yb_2O_3 oxidized for 200 hours at 900 °C. a) surface; and b) cross-section.

and region 4 is a particle of Yb_2O_3 present at alloy particle boundaries. Region 5, close to the oxide/metal interface is rich in Cr.

Similar microstructures were observed in the case of the other RE oxide dispersion containing steels. The mechanism most widely accepted at present, among those that have been put forth[3,10-19], to explain the reactive element effect, especially in so far as its effect on chromia growth, is the change in the ion species that diffuses predominantly. In rare earth free FeCr alloys, chromia growth takes place as a result of diffusion, of both oxygen and chromium[19], along grain boundaries, and the oxide layer is thick. On the other hand, in RE containing FeCr alloys, chromia growth is due to predominant oxygen ion diffusion[10]. The oxide layer is thin and plastic. Consequently the oxide layer is more adherent. The rare earth ions segregate to grain boundaries in the alloy and the oxide, close to the metal/oxide interface or to grain boundaries of the oxide. The ionic radii of the rare earths are significantly higher than that of the elements in the steel, Fe and Cr, and their presence at the alloy or oxide grain boundaries impedes cation diffusion. This in turn transforms regular anion diffusion into the predominant diffusing species and thus determines oxide growth.

4. Conclusions

Rare earth oxide additions to AISI 304L stainless steels decreased overall weight gain due to oxidation. The influence of RE additions on oxidation behavior remained effective for up to 200 hours. The results of microscopic examination of oxidized surfaces and sections gave further evidence that oxide growth on RE containing steels was by predominant oxygen diffusion.

Ackowlegments

The Authors wish to thank FAPESP for the financial support given through Project N° 01/13748-6.

References

1. Sttot FH. Influence of alloy additions on oxidation. *Materials Science and Technology*. 1989; 5:734.
2. Pettit FS, Goward GW. High temperature corrosion and use of coatings for protection. In: *Superalloys source book*, ASM. 1981. p. 170-186.

3. Hou PY, Stringer J. The effect of surface-applied reactive metal oxides on the high temperature oxidation of alloys. *Materials Science and Engineering*. 1987; 87:295.
4. Pillis MF, Ramanathan LV. Effect of Processing Technique on Microstructure and Oxidation Behavior of Rare Earth Oxide Dispersion Containing Steels. *Key Engineering Materials*. 2001; 189-191:322.
5. Pillis MF, Ramanathan LV. Effect of alloying additions and preoxidation on high temperature sulphidation resistance of iron-chromium alloys. *Surface Engineering*. 2006; 22(2):129.
6. Brossard J-M, Balmain J, Cresus J, Bonnet G. Characterization of thin solid films containing yttrium formed by electrogeneration of base for high temperature corrosion applications. *Surface and Coatings Technology*. 2004; 185:275.
7. Zhu L, Peng X, Yan J, Wang F. Oxidation of a Novel Chromium Coating with CeO_2 Dispersions. *Oxidation of Metals*. 2004; 62(5/6):411.
8. Chevalier S, Bonnet G, Larpin JP. Metal-organic chemical vapour deposition of Cr_2O_3 and Nd_2O_3 coatings. Oxide growth kinetics and characterization. *Applied Surface Science*. 2000; 167:125.
9. Pillis MF, de Araújo EG, Ramanathan LV. Effect of Addition of Rare Earth Oxide Concentrates on Oxidation Behavior of AISI 304L Stainless Steel. *TMS Letters*; 2004. p. 57.
10. Jedlinski J, Mrowec S. The influence of implanted yttrium on the oxidation behavior of -Ni-Al. *Materials Science and Engineering*. 1987; 87:281.
11. Rhys-Jones TN, Grabke HJ, Kudielka H. The effects of various amounts of alloyed cerium and cerium oxide on the high temperature oxidation of Fe-10Cr and Fe-20Cr alloys. *Corrosion Science*. 1987; 27(1):49.
12. Moon DP. Role of reactive elements in alloy protection. *Materials Science and Technology*. 1989; 5:754.
13. Cotell CM, Yurek GJ, Hussey RJ, Mitchell DF, Graham MJ. The influence of grain-boundary segregation of Y in Cr_2O_3 on the oxidation of Cr metal. *Oxidation of Metals*. 1990; 34(3/4):173.
14. Whittle DP, Stringer J. Improvements in high temperature oxidation resistance by additions of reactive elements or oxide dispersions. *Philosophical. Transactions of the Royal Society of London*. 1980; A295:309.
15. Pieraggi B, Rapp RA. Chromia scale growth in alloy oxidation and the reactive element effect. *Journal of the Electrochemical Society*. 1993; 140(10):2844.
16. Rhys-Jones TN, Grabke HJ. Use of cerium and cerium oxide additions to improve high temperature oxidation behaviour of Fe-Cr alloys. *Materials Science and Technology*. 1988; 4:446.
17. Pilling NB, Bedworth RE. The oxidation of metals at high temperatures. *Journal of the Institute of Metals*. 1923; 29:529.
18. Yurek GJ. Mechanisms of diffusion-controlled high-temperature oxidtion of metals. In: *Corrosion Mechanisms*. revised ed. New York: Marcel Dekker; 1987. p. 397-446.
19. Banovic SW, Dupont JN, Marder AR. High temperature sulfidation behavior of low Al iron-aluminium compositions. *Scripta Materialia*. 1998; 38(12):1763.